



Equilibrium solubility of pure and mixed 3,5-dinitrobenzoic acid and 3-nitrobenzoic acid in supercritical carbon dioxide

Zhao Tang, Jun-su Jin*, Xiang-yun Yu, Ze-ting Zhang, Hong-tao Liu

College of Chemical Engineering, Beijing University of Chemical Technology, 15 Beisanhuan East Road, Beijing 100029, China

ARTICLE INFO

Article history:

Received 8 October 2010
Received in revised form 26 January 2011
Accepted 30 January 2011
Available online 18 February 2011

Keywords:

Solubility
3,5-Dinitrobenzoic acid
3-Nitrobenzoic acid
Mixture
Supercritical carbon dioxide

ABSTRACT

The solid solubility of pure 3,5-dinitrobenzoic acid (3,5-DNBA) and 3-nitrobenzoic acid (*m*-NBA) and their equal-weight mixture in supercritical carbon dioxide (SCCO₂) was measured using a flow-type apparatus at 308, 318, and 328 K and in the pressure range of 10.0–21.0 MPa. The solubility enhancement *SE* of mixed 3,5-DNBA and *m*-NBA in the ternary system has been observed. The mixture separation factor μ and the separation efficiency *HE* were investigated. A modified Kumar–Johnston (K–J) model was proposed for correlating the solubility of solid compounds in SCCO₂. The experimental solubility data of pure and mixed solutes in SCCO₂ were successful to be correlated by Chrastil model, the modified Adachi–Lu model, K–J model and new proposed model. Solubility data from 23 different solid compounds were taken from literature. The accuracy of the proposed model was evaluated by correlating 13 binary systems, 13 ternary systems, and 1 quaternary system. The modified K–J model satisfactorily correlated the experimental results for the solubility of all these compounds in SCCO₂ within 5.11% AARD.

© 2011 Elsevier B.V. All rights reserved.

1. Introduction

Supercritical fluid (SCF) technology has gained a rapid growth for the past few decades, and has been widely applied in food processing, pharmaceutical industries, separation processes, chemical reaction and a variety of extractions [1]. Carbon dioxide (CO₂) is a solvent of choice in SCF technology because it is inexpensive, nontoxic, readily available in relatively pure form, and has moderate critical constants (7.38 MPa and 304 K). Supercritical carbon dioxide (SCCO₂) has strong solvent power, high diffusivity and low viscosity. These unique properties make SCCO₂ an attractive solvent for many industrial separation and purification processes, especially in the pharmaceutical industry [2].

3,5-Dinitrobenzoic acid (3,5-DNBA) and 3-nitrobenzoic acid (*m*-NBA) are important pharmaceutical intermediate materials for the pharmaceutical industry. 3,5-DNBA is mainly used for the synthesis of sulfachrysoidine and the detection of ampicillin. *m*-NBA is used for the production of agricultural chemicals and dyes, in particular for the synthesis of procaine hydrochloride, procaine ammonium salts, and amino-nitro benzoic acid. These two aromatic compounds are similar in production and application processes, and benzoic acid is their common raw material in industry [3]. It reports that benzoic acid reacts with a three mole ratio of the BF₃·N₂O₅ complex in carbon tetrachloride in 36 h at 70 °C to form 3,5-DNBA (70% yield) and *m*-NBA (9.3% yield). The mixture products of 3,5-

DNBA and *m*-NBA should be separated before further reaction and preparation of single pure compound. Thus, it is a necessary step to separate the mixture of 3,5-DNBA and *m*-NBA in industry.

For the separation and purification of pharmaceutical materials using SCCO₂ extraction technology, it is important to determine the solubility of solid compounds in SCCO₂. Many recent literature have reviewed the solubility data of solid compounds in SCCO₂ [4,5]. However, no solubility data of pure or mixed 3,5-DNBA and *m*-NBA in SCCO₂ have been listed in previous literature.

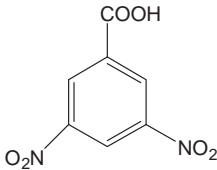
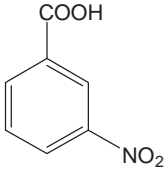
Because the experimental determination of the solubility of solid compounds in SCCO₂ at various temperatures and pressures is time consuming, modeling of the solubility data in SCCO₂ is essential. Models used for correlating the solubility data can be broadly classified as equation of state (EOS) based models and semi-empirical models [6,7]. EOS based models like cubic equation of state or perturbed equations need large and complicated computational methods and the knowledge of the solid properties (macroscopic critical properties and sublimation pressure are needed for cubic equations of state and molecular parameters for perturbed equations). These data are normally not available for many complex pharmaceutical compounds, which are determined by group contribution methods [8,9]. Due to several drawbacks, an error is produced in their estimations.

On the other hand, semi-empirical equations, like density based models, only need available independent variables like pressure, temperature and density of pure SCF instead of solid properties. They are based on simple error minimization. The only drawback is the semi-empirical character, which means that solubility data are needed [10]. Recently, many semi-empirical models such as

* Corresponding author. Tel.: +86 10 64434788; fax: +86 10 64436781.

E-mail addresses: jinjs@mail.buct.edu.cn, necwebber@yahoo.com.cn (J.-s. Jin).

Table 1
Chemical structures of solid compounds.

Compound	Formula	Molecular structure	T_m (K) ^a
3,5-Dinitrobenzoic acid	$C_7H_4N_2O_6$		479.2
3-Nitrobenzoic acid	$C_7H_5NO_4$		414.2

^a T_m is the melting point of compound searching from the website of Chem YQ.

Chrastil model [11], Méndez-Santiago and Teja model [12], Bartle model [13], Gordillo model [14], del Valle and Aguilera model [15], Adachi and Lu model [16], Sparks model [17], Kumar and Johnston (K–J) model [18], and Yu model [19] are used for correlating the solubility data of solid compounds in $SCCO_2$. However, it is still uncertain which is the best model to predict more accurately for the solubility data of solid solutes in $SCCO_2$, especially for the mixtures of solid solutes.

Thus, an excellent mathematical modeling of solubility data in SCF could provide better understanding of the dissolution phenomenon and can be used for solubility prediction at interested pressures and temperatures after measuring a minimum number of experimental data, which could speed up the development of SCF technology.

In this work, the solubility of pure and mixed 3,5-DNBA and *m*-NBA in $SCCO_2$ was measured at 308, 318, and 328 K over a pressure range from 10.0 to 21.0 MPa. The optimal operation for the separation of 3,5-DNBA and *m*-NBA using $SCCO_2$ extraction technology was investigated. The experimental solubility data were correlated by Chrastil model, the modified Adachi and Lu model, and K–J model. A modified semi-empirical model with four parameters based on K–J model was developed and used to correlate the solubility data of 25 different solid compounds from this work and literature.

2. Experimental methods

2.1. Chemicals and raw materials

Carbon dioxide (CAS 124-38-9) (more than 99.9% mass fraction) was purchased from Beijing Praxair Industrial Gas Co., Ltd.

3,5-DNBA ($C_7H_4N_2O_6$, CAS 99-34-3) and *m*-NBA ($C_7H_5NO_4$, CAS 121-92-6) with an assessed minimum mass purity of 99% (analytical purity) were purchased from Beijing Hengye Zhongyuan Chemical Co., Ltd. The chemical structures and melting points of solid compounds are shown in Table 1. All chemicals were used without further purification.

2.2. Experimental procedure

The solubility of 3,5-DNBA and *m*-NBA in $SCCO_2$ was measured using a dynamic flow technique with ultraviolet spectrophotometer analysis. A schematic diagram of the experimental apparatus is shown in Fig. 1.

CO_2 supplied to a high-pressure surge flask from a cylinder was pressurized by the compressor (Nova, model 5542121). High-pressure CO_2 entered into a preheating and mixing cell with a heating electric coil so that its temperature and pressure could reach to the operating condition. $SCCO_2$ entered into a high-pressure equilibrium cell with an available volume of 150 mL from the bottom consecutively, which was loaded 40 or 50 g of packed solute mixed with the glass beads and stainless steel sintered disks at both ends to prevent physical entrainment of undissolved solute. The high-pressure equilibrium cell was immersed in a constant-temperature stirred water bath with preheating coils (Chongqing Yinhe Experimental Instrument Corporation, model CS-530), which was controlled to ± 0.5 K by a temperature controller. The temperature and pressure in the cell was measured by a calibrated internal platinum resistance thermometer (Beijing Chaoyang Automatic Instrument Factory, model, XMT) and a calibrated pressure gauge (Heise, model CTUSA), respectively. The uncertainty for temperature measurement is ± 0.1 K, and that for pressure is ± 0.05 MPa.

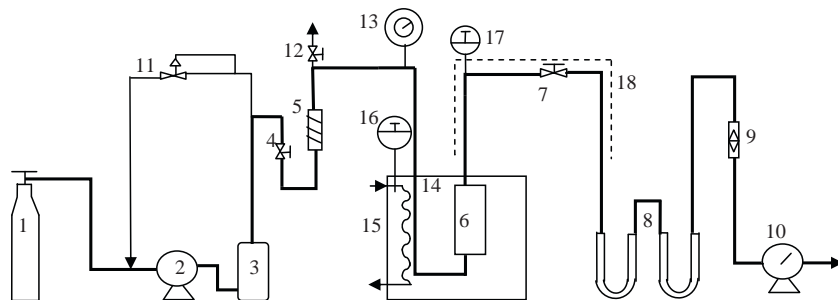


Fig. 1. Schematic diagram of the experimental apparatus: 1, CO_2 cylinder; 2, compressor; 3, high-pressure surge flask; 4, pressure regulating valve; 5, preheating and mixing cell; 6, high-pressure equilibrium cell; 7, decompression sampling valve; 8, U-shaped tube; 9, rotated flow meter; 10, wet-gas flow meter; 11, back pressure valve; 12, safety valve; 13, pressure gauge; 14, constant-temperature stirred water bath; 15, preheating coils; 16, temperature controller; 17, thermometer; 18, heating coils.

SCCO₂ flowed out from the top of the equilibrium cell through a decompression sampling valve (wrapped with heating coils) and the solid compound was separated from CO₂ and collected by two U-shaped tubes in turn. From experimental observation, nearly all the solute was collected in the first U-shaped tube, and scarcely little precipitated in the second U-shaped tube. 3,5-DNBA is hardly soluble in water and very soluble in ethanol, while *m*-NBA is both soluble in water or ethanol. As a result, the solvent used to wash the analytes in the U-shaped tubes was the mixed solvent of ethanol and water (the volume ratio of ethanol and water = 1:3). The total volume of CO₂ released during the experiment was measured by a calibrated wet gas flow meter (Changchun Instrument Factory, model LML-2) with an uncertainty of ±0.01 L at room temperature and atmospheric pressure.

To make sure the reliability of the experimental procedure, the equilibrium time and the suitable flow rate of CO₂ was determined, respectively. The flow rate experiments with a rotated flow meter were carried out before. The results showed that when the flow rate of CO₂ was in the range of 0.3–1.0 L min⁻¹, the equilibrium of system would be maintained. The average flow rate of 0.6 L min⁻¹ in this work was adopted. At a suitable flow rate of CO₂, the solubility of solutes was measured after 20, 30, 40, 50, and 60 min, respectively. The results showed that the solubility was nearly invariable after 30 min, which shows that the system had reached equilibrium. Therefore, all of the data were measured after 30 min.

2.3. Analytical methods and solubility measurements

UV spectrophotometer (UNICO, model UV-2100) method was used to analyze the amount of solutes collected in the U-shaped tubes. The reference solution was the mixed solvent of ethanol and water (the volume ratio of ethanol and water = 1:3). The maximum UV absorption λ_{max} of the sample was detected at a wavelength of 263 nm for 3,5-DNBA and 268 nm for *m*-NBA, respectively. A calibration curve was used to establish the concentration of solute with the regression coefficient better than 0.9995. The solubility of solute was determined by the concentration of solute and the flow volume of SCCO₂, and the solubility of solute in mole fraction was calculated according to the following formula:

$$y = \frac{S \times M_1}{S \times M_1 + \rho \times M_2} \quad (1)$$

where *S* is the solubility of solute (g L⁻¹), *M*₁ and *M*₂ are the molecular weights of CO₂ and solute (g mol⁻¹), respectively, *ρ* is the density of CO₂ at room temperature and normal atmospheric pressure (g L⁻¹), and *y* is the mole fraction solubility of the solute.

For the solubility measurements of mixed 3,5-DNBA and *m*-NBA in SCCO₂, the cumulative absorbance was resulted from the comprehensive contribution of both 3,5-DNBA and *m*-NBA. Thus, each composition of solutes in the ternary system (3,5-DNBA + *m*-NBA + SCCO₂) was determined by an absorbency measurement at both wavelengths of 268 nm (the maximum wavelength of *m*-NBA) and 237 nm (obtained by detecting the wavelength to acquire a maximum absorption difference with the absorption at 268 nm) using UV spectrophotometer. Consequently, the solubility of each solute was calculated by a least-squares regression from the relative absorbency at both wavelengths.

The reliability of the experimental apparatus was verified by measuring the solubility of solid solutes in our previous work [20,21]. Each reported data point in this work was the average of at least three replicated sample measurement to ensure the accuracy. The uncertainty of each measurement was within ±5%.

3. Theoretical section

3.1. Empirical models

Chrastil model [11] is one of the most frequently used density-based models, which indicates that the relationship between the solute solubility (*S*, g L⁻¹) in SCF and the solvent density (*ρ*₁, g L⁻¹) and temperature (*T*, K) as:

$$\ln S = A_0 \ln \rho_1 + \frac{A_1}{T} + A_2 \quad (2)$$

where *A*₀–*A*₂ are the model constants that can be estimated from experimental solubility data in SCF. *A*₀ is an association constant describes the number of SCF molecules in the solvated complex, *A*₁ is a function of the enthalpy of salvation and vaporization, and *A*₂ is a function of the association number and molecular weights of the solute and SCF.

Adachi and Lu [16] modified Chrastil's model to better model the solubility of triglycerides. Chrastil assumed the association number *A*₀ to be constant and independent of density. Adachi and Lu changed the association number *A*₀ to a second-order polynomial of density. They proposed that the association constant *A*₀ could be expressed as *A*₀ = *e*₀ + *e*₁*ρ*₁ + *e*₂*ρ*₁². They found that a significant reduction in variation between experimental and calculated solubility data could be achieved for some systems by modifying the association number *A*₀.

Sparks et al. [17] found that Adachi and Lu modified the term for the association constant *A*₀ in Chrastil model so that it became a quadratic function of density. However, when values of the modified *A*₀ were calculated for several solid-SCCO₂ systems [16] and plotted against reduced density, an interesting trend can be observed. Though *A*₀ was generated from a quadratic function, the change of *A*₀ with density is somewhat linear for each compound. Therefore, Adachi and Lu model can be simplified (with insignificant loss of efficacy) to the following form as *A*₀ = *e*₀ + *e*₁*ρ*₁. Therefore, the solubility of solute (*S*, g L⁻¹) in SCF can be correlated to the solvent density (*ρ*₁, g L⁻¹) and temperature (*T*, K) by the modified Adachi and Lu model:

$$\ln S = (B_0 + B_1 \rho_1) \ln \rho_1 + \frac{B_2}{T} + B_3 \quad (3)$$

where *B*₀–*B*₃ are the model constants.

Kumar and Johnston [18] pointed out that the linear relationships observed between ln *y*₂ and ln *ρ*₁ and in some cases between ln *y*₂ and *ρ*₁ are system dependent and neither can be validly generalized. Similar to Eq. (2), the linear expression between ln *y*₂ and *ρ*₁ could be given as:

$$\ln y_2 = C_0 \rho_1 + \frac{C_1}{T} + C_2 \quad (4)$$

where *y*₂ is the mole fraction solubility of solute in SCF, *ρ*₁ (g L⁻¹) is the solvent density, *T* (K) is temperature, and *C*₀–*C*₂ are the model constants.

K–J model is expressed with three adjustable parameters (*C*₀, *C*₁ and *C*₂) in Eq. (4). The value of *C*₁ is related to the total heat Δ*H*_{total} (heat of solvation Δ*H*_{sol}, plus heat of vaporization of the solute Δ*H*_{vap}), which cannot be changed random in the experiment. Parameter *C*₂ is a constant only acquired from the experimental data. Take into account the viewpoints of Adachi and Lu and Sparks et al. [16,17], the adjustable parameter *C*₀ should be related with density. Thus, *C*₀ is defined in this work as *C*₀ = *D*₀ + *D*₁ ln *ρ*₁, which is linear with ln *ρ*₁, rather than a constant, as K–J model simulated.

The following empirical model was proposed for the solubility of solid solutes in SCF as:

$$\ln y_2 = (D_0 + D_1 \ln \rho_1) \rho_1 + \frac{D_2}{T} + D_3 \quad (5)$$

Table 2
The mole fraction solubility of pure (y_b) and mixed (y_t) 3,5-DNBA and *m*-NBA in SCCO₂ with the solubility enhancement *SE*, mixture separation factor μ and the separation efficiency *HE* at temperatures of 308, 318, and 328 K and a pressure range of 10.0–21.0 MPa.

T (K)	p (MPa)	ρ_1^a (g/L)	3,5-DNBA			<i>m</i> -NBA			μ	<i>HE</i> (%)
			$10^6 \cdot y_b$	$10^6 \cdot y_t$	<i>SE</i> (%)	$10^6 \cdot y_b$	$10^6 \cdot y_t$	<i>SE</i> (%)		
308	10.0	714.84	0.58	1.22	110	7.21	7.43	3	6.09	85.90
	12.0	768.42	0.73	2.27	211	14.32	16.85	18	7.42	88.13
	15.0	816.06	0.94	2.69	186	19.44	27.56	42	10.25	91.11
	18.0	848.87	1.08	3.12	189	24.08	33.55	39	10.75	91.49
	21.0	874.40	1.09	3.45	217	25.36	37.71	49	10.93	91.62
			Average		183			30	9.09	89.65
318	10.0	502.57	0.48	0.51	6	3.33	4.43	33	8.69	89.68
	12.0	659.73	1.17	2.45	109	14.94	22.92	53	9.36	90.34
	15.0	743.17	1.69	3.86	128	34.34	40.68	18	10.54	91.33
	18.0	790.18	2.14	5.09	138	47.03	62.60	33	12.30	92.48
	21.0	823.71	2.30	7.11	209	60.68	74.61	23	10.49	91.30
			Average		118			32	10.27	91.03
328	10.0	326.40	0.44	0.45	2	1.44	1.71	19	3.80	79.17
	12.0	506.85	1.31	1.50	15	10.38	12.02	16	8.01	88.91
	15.0	654.94	2.65	4.89	85	46.19	56.08	21	11.47	91.98
	18.0	724.13	3.57	7.23	103	79.59	90.02	13	12.45	92.57
	21.0	768.74	4.21	9.82	133	109.86	121.53	11	12.38	92.52
			Average		67			16	9.62	89.03

^a ρ_1 is the density of pure CO₂ at different experimental pressures and temperatures, which is obtained from the NIST fluid property database.

Table 3
Correlation parameters for the solubility of 3,5-DNBA and *m*-NBA in SCCO₂ for the binary and ternary systems.

	Models	Correlation parameters	AARD (%)
Binary system 3,5-DNBA	Chrastil model	$A_0 = 2.7982; A_1 = -8755.6; A_2 = -2.0838$	4.75
	Modified Adachi–Lu model	$B_0 = 1.5243; B_1 = 0.000314; B_2 = -9019.9; B_3 = 5.6113$	3.20
	K–J model	$C_0 = 0.004996; C_1 = -9191.4; C_2 = 11.8634$	5.03
	Modified K–J model	$D_0 = 0.02324; D_1 = -0.002476; D_2 = -8999.7; D_3 = 9.8820$	3.22
	<i>m</i> -NBA	Chrastil model	$A_0 = 5.3236; A_1 = -10789.4; A_2 = -9.6893$
Modified Adachi–Lu model		$B_0 = 2.9892; B_1 = 0.000575; B_2 = -11273.7; B_3 = 4.4120$	5.42
K–J model		$C_0 = 0.009501; C_1 = -11612.8; C_2 = 19.0637$	9.51
Modified K–J model		$D_0 = 0.04597; D_1 = -0.004948; D_2 = -11229.8; D_3 = 15.1038$	5.10
Ternary system 3,5-DNBA	Chrastil model	$A_0 = 4.0159; A_1 = -8004.1; A_2 = -11.6981$	12.81
	Modified Adachi–Lu model	$B_0 = 0.4904; B_1 = 0.000869; B_2 = -8735.4; B_3 = 9.5978$	8.71
	K–J model	$C_0 = 0.007270; C_1 = -8732.9; C_2 = 9.5642$	8.57
	Modified K–J model	$D_0 = 0.00962; D_1 = -0.000318; D_2 = -8708.2; D_3 = 9.3095$	8.54
	<i>m</i> -NBA	Chrastil model	$A_0 = 5.3242; A_1 = -10259.8; A_2 = -11.1475$
Modified Adachi–Lu model		$B_0 = 2.6261; B_1 = 0.000665; B_2 = -10819.6; B_3 = 5.1503$	8.60
K–J model		$C_0 = 0.009522; C_1 = -11104.0; C_2 = 17.6731$	11.72
Modified K–J model		$D_0 = 0.03933; D_1 = -0.004044; D_2 = -10790.9; D_3 = 14.4368$	8.58

Table 4
Data references for the compounds considered in this study.

No.	Compound	Formula	T (K)	P (MPa)	N	Reference
1	5-Sulfosalicylic acid	C ₇ H ₆ O ₄ S	308–328	8.0–21.0	15	[27]
2	<i>p</i> -Aminobenzoic acid	C ₇ H ₇ NO ₂	308–328	8.0–21.0	15	[27]
3	Ethyl <i>p</i> -hydroxybenzoate	C ₉ H ₁₀ O ₃	308–328	8.0–21.0	15	[28]
4	Ethyl <i>p</i> -aminobenzoate	C ₉ H ₁₁ NO ₂	308–328	8.0–21.0	15	[28]
5	<i>p</i> -Toluenesulfonamide	C ₇ H ₉ NO ₂ S	308–328	11.0–21.0	15	[29]
6	Sulfanilamide	C ₆ H ₈ N ₂ O ₂ S	308–328	11.0–21.0	15	[29]
7	Benzoic acid	C ₇ H ₆ O ₂	308–328	10.1–28.0	18	[30]
8	Salicylic acid	C ₇ H ₆ O ₃	308–328	10.1–28.0	18	[30]
9	Acetylsalicylic acid	C ₉ H ₈ O ₄	308–328	10.1–28.0	18	[30]
10	Medroxyprogesterone acetate	C ₂₄ H ₃₄ O ₄	308–348	12.2–35.5	40	[31]
11	Cyproterone acetate	C ₂₄ H ₂₉ ClO ₄	308–348	12.2–35.5	40	[31]
12	Disperse Red 73	C ₁₈ H ₁₆ N ₆ O ₂	343–383	12.0–28.0	15	[32]
13	Disperse Yellow 119	C ₁₅ H ₁₃ N ₅ O ₄	343–383	12.0–28.0	15	[32]
14	Cholesteryl benzoate	C ₃₄ H ₅₀ O ₂	308.15–328.15	12.0–24.0	17	[33]
15	Cholesteryl butyrate	C ₃₁ H ₅₂ O ₂	308.15–328.15	12.0–24.0	17	[33]
16	Mono- <i>tert</i> -butyl ethers of glycerol	C ₇ H ₁₆ O ₃	313.15–348.15	8.0–20.0	14	[34]
17	Di- <i>tert</i> -butyl ethers of glycerol	C ₁₁ H ₂₄ O ₆	313.15–348.15	8.0–20.0	14	[34]
18	Hexachlorobenzene	C ₆ Cl ₆	308–328	9.0–24.06	15	[35]
19	Pentachlorophenol	C ₆ Cl ₅ OH	308–328	9.0–24.06	15	[35]
20	1,10-Decanediol	C ₁₀ H ₂₂ O ₂	308–318	16.38–30.71	10	[36]
21	Benzoic acid	C ₇ H ₆ O ₂	308–318	16.38–30.71	10	[36]
22	Phenanthrene	C ₁₄ H ₁₀	308–318	10.31–23.91	10	[37]
23	Anthracene	C ₁₄ H ₁₀	308–318	10.31–23.91	10	[37]

Table 5
Correlation parameters for the solubility of compounds in SCCO₂ using the modified K–J model.

No.	Compound	D_0	D_1	D_2	D_3
Binary system					
1	5-Sulfosalicylic acid	1.4400e-2	-1.7089e-3	-1730.98	-10.1339
2	<i>p</i> -Aminobenzoic acid	9.1885e-3	-9.3986e-4	-2079.81	-8.0072
3	Ethyl <i>p</i> -hydroxybenzoate	4.2332e-2	-5.1802e-3	-4446.84	-1.2031
4	Ethyl <i>p</i> -aminobenzoate	5.3548e-2	-6.4727e-3	-4138.20	-2.0514
5	<i>p</i> -Toluenesulfonamide	-3.1718e-3	7.5725e-4	-3407.34	-0.9067
6	Sulfanilamide	-4.9720e-3	9.6288e-4	-4658.22	-1.4730
7	Benzoic acid	5.9106e-2	-7.0287e-3	-5224.67	0.9408
8	Salicylic acid	1.0870e-2	-7.8654e-4	-5404.26	4.7463
9	Acetylsalicylic acid	-4.0431e-3	1.3068e-3	-5947.86	6.2620
10	Medroxyprogesterone acetate	-4.3570e-2	6.7706e-3	-5125.57	5.3012
11	Cyproterone acetate	-6.2890e-2	9.2829e-3	-2611.14	-0.5895
12	Disperse Red 73	3.2045e-2	-3.8610e-3	-4080.03	-3.9635
13	Disperse Yellow 119	1.8634e-2	-1.8282e-3	-6815.18	3.0222
Ternary system					
1	5-Sulfosalicylic acid	1.0395e-2	-1.2122e-3	-1428.35	-10.4810
	<i>p</i> -Aminobenzoic acid	1.0750e-2	-1.2635e-3	-1259.46	-10.1108
2	Ethyl <i>p</i> -hydroxybenzoate	6.1928e-2	-7.6820e-3	-6028.82	2.4032
	Ethyl <i>p</i> -aminobenzoate	5.7304e-2	-6.9336e-3	-4320.61	-1.7311
3	<i>p</i> -Toluenesulfonamide	-1.1884e-2	2.1132e-3	-5480.40	5.0330
	Sulfanilamide	7.3099e-3	-7.7005e-4	-3210.28	-6.3997
4	Benzoic acid	4.9411e-2	-5.7279e-3	-5143.15	1.4849
	Salicylic acid	3.1613e-2	-3.3639e-3	-5665.65	3.6448
5	Benzoic acid	3.8320e-2	-4.2100e-3	-5917.65	4.8504
	Acetylsalicylic acid	2.7257e-2	-2.5545e-3	-7178.55	7.1142
6	Salicylic acid	2.2175e-2	-2.1601e-3	-5730.32	4.3350
	Acetylsalicylic acid	-8.9059e-4	1.0116e-3	-6546.61	7.7525
7	Medroxyprogesterone acetate	-5.4864e-2	8.0335e-3	-3744.61	3.5130
	Cyproterone acetate	-5.9721e-2	8.6205e-3	-3076.02	1.6648
8	Disperse Red 73	1.6268e-2	-1.6132e-3	-4501.55	-2.2870
	Disperse Yellow 119	4.0710e-3	-8.8115e-5	-4737.14	0.5843
9	Cholesteryl benzoate	7.2903e-2	-8.3326e-3	-7231.02	0.3612
	cholesteryl butyrate	7.9802e-2	-9.0984e-3	-7724.27	-1.8192
10	Mono- <i>tert</i> -butyl ethers of glycerol	4.4042e-2	-5.4756e-3	-2553.57	-3.2763
	Di- <i>tert</i> -butyl ethers of glycerol	3.0442e-2	-3.7524e-3	-1976.88	-4.2448
11	Hexachlorobenzene	1.1040e-1	-1.4062e-2	280.49	-24.4688
	Pentachlorophenol	3.7362e-2	-4.3201e-3	-4792.20	0.2005
12	1,10-Decanediol	-1.8093e-1	2.3854e-2	-6621.34	30.0567
	Benzoic acid	5.4004e-3	-9.3819e-5	-4289.00	3.9268
13	Phenanthrene	7.2043e-2	-8.5736e-3	-5571.79	-0.6192
	Anthracene	9.6274e-2	-1.1723e-2	-5125.50	-7.4187
Quaternary system					
1	Benzoic acid	5.2139e-2	-5.9750e-3	-5879.24	3.1266
	Salicylic acid	5.5034e-2	-6.3209e-3	-6664.57	4.0592
	Acetylsalicylic acid	4.9354e-2	-5.3955e-3	-7475.26	5.7293

where D_0 – D_3 are the model constants, y_2 is the mole fraction solubility of solute in SCF, ρ_1 (g L⁻¹) is the density of pure solvent at different experimental pressures and temperatures, and T (K) is temperature.

3.2. Methodology

The average absolute relative deviation (AARD) of the model from experimental data was calculated according to the following formula:

$$\text{AARD}(\%) = \frac{100}{n} \sum_{i=1}^n \frac{|y_{\text{cal}} - y_{\text{exp}}|}{y_{\text{exp}}} \quad (6)$$

where y_{cal} is the calculated value of the mole fraction solubility of solute, y_{exp} is the experimental value of the mole fraction solubility of solute, n is the number of experimental points. The name and version of software that we used to fit the experimental and calculated data was Microsoft Office Excel 2007.

4. Results and discussions

For the binary system (3,5-DNBA/*m*-NBA+SCCO₂) and the ternary system (3,5-DNBA+*m*-NBA+SCCO₂) (the mass ratio of

3,5-DNBA and *m*-NBA = 1:1), the mole fraction solubility data of solutes in SCCO₂ at 308, 318, and 328 K over the pressures range of 10.0–21.0 MPa are all listed in Table 2. The density of CO₂ obtained from the NIST fluid property database is also shown in Table 2. In this work, Chrastil model, the modified Adachi and Lu model, K–J model, and the modified K–J model proposed in our work, Eqs. (2)–(5), were used to correlate the solubility data of solids in SCCO₂.

4.1. Solubility in the binary system

As shown in Table 2 and Fig. 2, the equilibrium solubility of each solid solute increases with increasing pressure at three temperatures (308, 318, and 328 K). It can attribute to the increase of solvent's density with increasing pressure and the specific stronger interactions between solute and solvent molecules at higher pressure. The crossover pressure regions have been observed, as shown in Fig. 2. They are from 10.5 to 11.2 MPa and 11.2–13.0 MPa for 3,5-DNBA and *m*-NBA, respectively. The crossover phenomena could be attributed to the competitions between solute's vapor pressure and solvent's density, whose dependences on temperature are in opposite directions. Below the crossover pressure region, the density effect, sensitive to the solute's vapor pressure, is dominant so that the solute is more soluble at low temperature. However, above the

Table 6
Comparison of AARD of the K–J model, modified K–J model and the models discussed from literature.

No.	Compound	Models from literature ^a	K–J ₁ ^b	K–J ₂ ^c
Binary system				
1	5-Sulfosalicylic acid	Chrastil 3.48	5.95	3.54
2	<i>p</i> -Aminobenzoic acid	Chrastil 6.39	6.49	5.26
3	Ethyl <i>p</i> -hydroxybenzoate	Chrastil 4.62	14.79	5.68
4	Ethyl <i>p</i> -aminobenzoate	Chrastil 3.26	19.32	4.02
5	<i>p</i> -Toluenesulfonamide		1.79	1.79
6	Sulfanilamide		4.19	4.07
7	Benzoic acid		3.00	1.94
8	Salicylic acid		1.76	1.71
9	Acetylsalicylic acid		1.65	1.63
10	Medroxyprogesterone acetate		15.38	9.24
11	Cyproterone acetate		18.48	11.17
12	Disperse Red 73	Chrastil 9; MST 13	11.81	9.28
13	Disperse Yellow 119	Chrastil 11; MST 13	9.81	9.10
	Average ^d		8.80	5.26
Ternary system				
1	5-Sulfosalicylic acid	Chrastil 4.87	5.69	4.75
	<i>p</i> -Aminobenzoic acid	Chrastil 4.71	4.68	4.59
2	Ethyl <i>p</i> -hydroxybenzoate	Chrastil 5.01	23.35	6.37
	Ethyl <i>p</i> -aminobenzoate	Chrastil 4.52	20.59	5.62
3	<i>p</i> -Toluenesulfonamide	Chrastil 6.6; MST 8.5	3.56	2.73
	Sulfanilamide	Chrastil 1.8; MST 6.3	1.80	1.57
4	Benzoic acid		2.15	1.33
	Salicylic acid		2.30	2.12
5	Benzoic acid		3.11	2.99
	Acetylsalicylic acid		2.87	2.86
6	Salicylic acid		1.51	1.44
	Acetylsalicylic acid		2.72	2.65
7	Medroxyprogesterone acetate		21.25	16.38
	Cyproterone acetate		22.84	17.96
8	Disperse Red 73	Chrastil 10; MST 10	8.46	8.18
	Disperse Yellow 119	Chrastil 11; MST 11	7.76	7.82
9	Cholesteryl benzoate	Chrastil 6.3; MST 6.3; Bartle 5.5; PR-EOS 9.7	7.24	4.91
	Cholesteryl butyrate	Chrastil 4.9; MST 5.8; Bartle 4.9; PR-EOS 9.0	8.47	5.95
10	Mono- <i>tert</i> -butyl ethers of glycerol	Bartle 14.56	16.96	10.30
	Di- <i>tert</i> -butyl ethers of glycerol	Bartle 13.88	14.01	6.20
11	Hexachlorobenzene		6.89	5.60
	Pentachlorophenol		3.60	3.83
12	1,10-Decanediol	PR-EOS 9.1	5.12	4.77
	Benzoic acid	PR-EOS 9.8	1.52	1.52
13	Phenanthrene		6.14	2.44
	Anthracene		9.28	4.58
Quaternary system				
1	Benzoic acid		3.48	2.78
	Salicylic acid		2.60	1.41
	Acetylsalicylic acid		3.03	2.57
	Average ^e		7.69	5.04
	Total average ^f		8.03	5.11

^a Chrastil is Chrastil model; MST is Méndez-Santiago and Teja model; Bartle is Bartle model; PR-EOS is the Peng–Robinson equation of state.

^b K–J₁ is K–J model.

^c K–J₂ is the modified K–J model.

^d The average values of AARD for the binary system.

^e The average values of AARD for the ternary and quaternary systems.

^f The total average values of AARD for all systems.

crossover pressure region, solute's vapor pressure becomes dominant at higher temperature and the density of the solvent turns less sensitive to the solute's vapor pressure. At the crossover point, these two competitive factors effect rather.

The solubility data in Table 2 obtained in this study indicate that 3,5-DNBA has lower solubility in SCCO₂ than *m*-NBA. The difference between 3,5-DNBA and *m*-NBA is the increase of a nitro-functional group by comparing their molecular structure. Therefore, the centrosymmetric dimmers are present in the crystal of pure 3,5-DNBA [22], which is the case in the structures of diversity of *m*-NBA. Two polymorphic groups make 3,5-DNBA easier to be a potential hydrogen bond acceptor, which indicates that 3,5-DNBA has higher polarity than *m*-NBA. CO₂ exhibits both non-polar tendencies (low dielectric constant) and 'polar' properties (Lewis acidity, strong quadrupole moment). Due to its structural symmetry, CO₂ does not have a dipole moment, but it does have a substantial quadrupole

moment that operates over a much shorter distance than dipolar interactions. Although CO₂ molecules present a quadrupolar effect, the polarity of CO₂ is still smaller than most of polar solvents [23]. Based on the "like-dissolves-like" principle, the more polar a solute, the lower solubility in CO₂, the strong polar molecular interaction among the polar 3,5-DNBA molecules impacts on the molecular interaction between 3,5-DNBA and CO₂, which leads to its lower solubility.

In addition, according to the experimental data of the Table 2, at 328 K, the mole solubility of pure *m*-NBA increases from 1.44×10^{-6} to 109.86×10^{-6} significantly; however, the mole solubility of the pure 3,5-DNBA increases from 0.44×10^{-6} to 4.21×10^{-6} . McHugh and Paulaitis illustrated the solubility behavior of a solid in SCCO₂ [24]. As they said, A vicinity of upper critical end point (UCEP) of the binary mixture (*m*-NBA + SCCO₂) can be reached, which results to the change in solubility with pressure becomes more drastic.

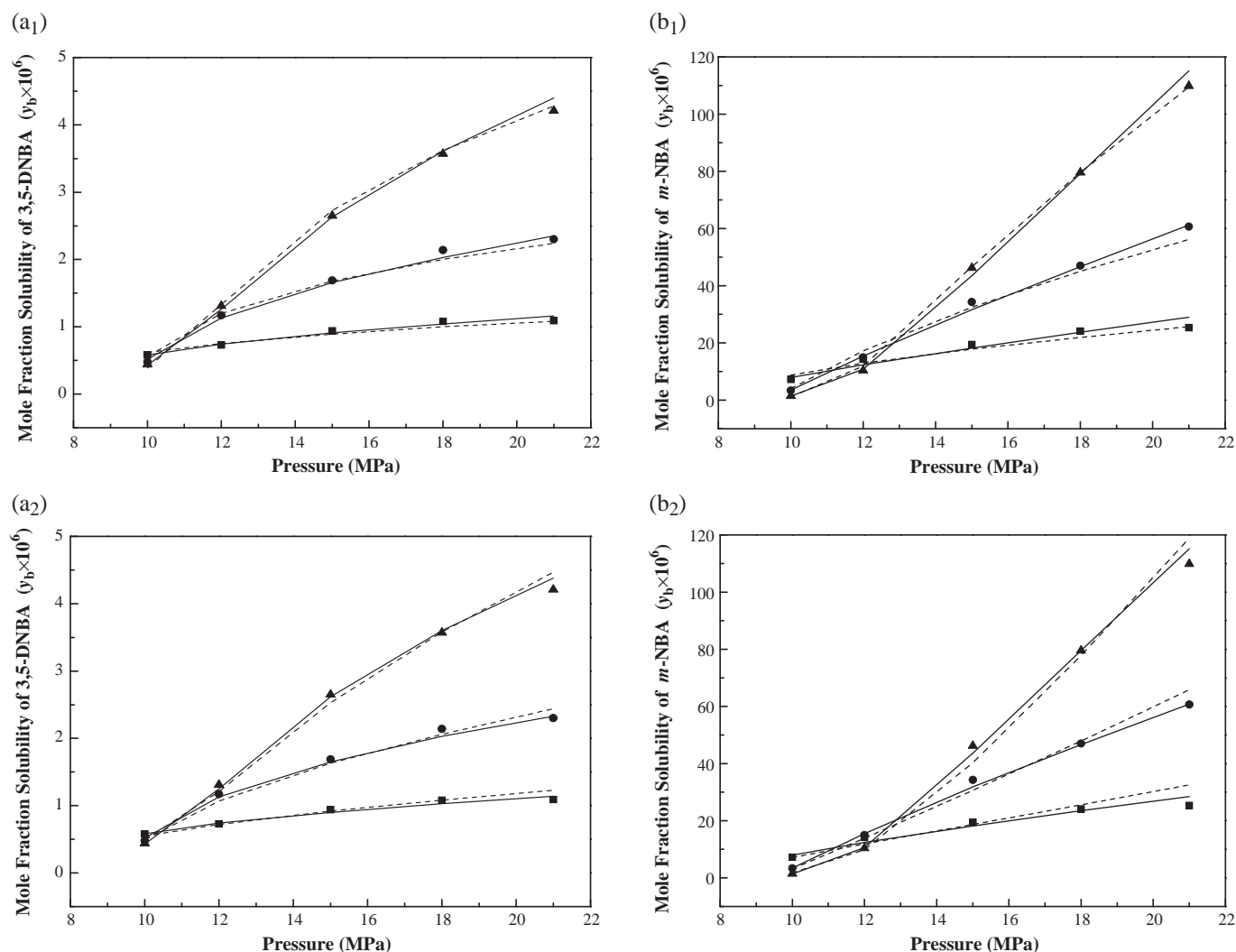


Fig. 2. Experimental solubility data (Table 2) in the binary system in mole fraction (y_b) with pressure (a) 3,5-DNBA + SCCO₂ and (b) *m*-NBA + SCCO₂ (■) 308 K; (●) 318 K; (▲) 328 K. (a₁ and b₁) The dash lines and solid lines are model correlations based on Chrastil model and the modified Adachi–Lu model, respectively (Eqs. (2) and (3)) and (a₂ and b₂) The dash lines and solid lines are model correlations based on K–J model and the modified K–J model, respectively (Eqs. (4) and (5)) and all the correlation parameters are given in Table 3.

4.2. Solubility in the ternary system

The effect of pressure and temperature on the solubility of each solid solute in the ternary systems follows the same trend as that in the binary systems, as shown in Table 2 and Fig. 3. In the ternary system, the crossover pressure region transferred to 12.0–13.0 MPa for 3,5-DNBA and 12.0–13.5 MPa for *m*-NBA, respectively.

In order to make an easier comparison of solubility data between the binary and ternary systems, here the solubility enhancement *SE* was defined as the percentage relative deviation of the ternary solubility from the binary solubility of the component at the same pressure and temperature:

$$SE(\%) = \frac{y_t - y_b}{y_b} \times 100 \quad (7)$$

where y_b and y_t are the mole fraction solubility of solutes in SCCO₂ in the binary and ternary system, respectively.

The values of *SE* of these two solutes in the ternary system are listed in Table 2. The average values of *SE* of 3,5-DNBA at 308, 318, and 328 K are up to 183, 118, and 67, respectively. And the corresponding values of *SE* of *m*-NBA are 30, 32, and 16, respectively. Kurnik and Reid [25] have explained the solubility enhancement in mixed-solid systems in terms of the location of the UCEP. They

argued that the higher solubility would be expected in the ternary system at same temperature because it is closer to the UCEP when in comparison to the binary system.

Comparing the values of *SE* of these two solutes, it indicates that the solubility enhancement of 3,5-DNBA is higher than *m*-NBA in the ternary system, which were also observed similarly on other solid mixtures [25,26]. The molecular interaction between these two solutes and CO₂ may result in the difference. Both 3,5-DNBA and *m*-NBA have stronger molecular polarity than CO₂. Regarding in the ternary system, one solid solute played a “co-solvent” role. Hence two solutes are liable to form the hydrogen bond, which leads to the enhancement of their solubility. However, due to the presence of two polar nitro-functional groups, 3,5-DNBA is a relatively stronger proton donor as well as proton acceptor than *m*-NBA with one nitro-functional group. Therefore, the solubility enhancement of 3,5-DNBA is higher than *m*-NBA in the ternary system.

4.3. Mixture separation

The effect of operating conditions on selectivity is necessary for the optimal design of a separation process. The appropriate condition for separating these two solids in SCCO₂ is confirmed by

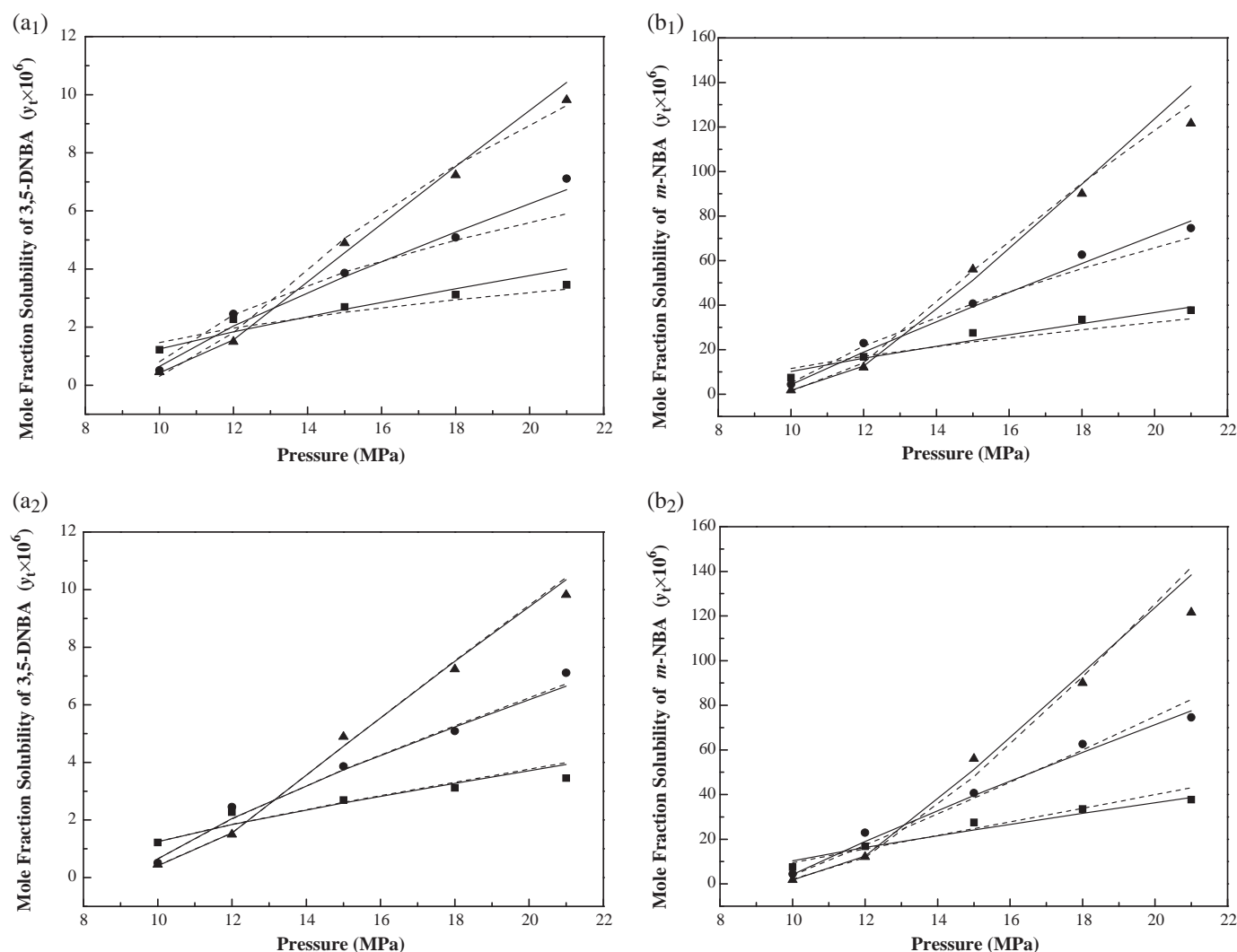


Fig. 3. Experimental solubility data (Table 2) in the ternary system (3,5-DNBA + *m*-NBA + SCCO₂) in mole fraction (y_t) with pressure (a) 3,5-DNBA and (b) *m*-NBA (■) 308 K; (●) 318 K; (▲) 328 K. (a₁ and b₁) The dash lines and solid lines are model correlations based on Chrastil model and the modified Adachi–Lu model, respectively (Eqs. (2) and (3)) and (a₂ and b₂) The dash lines and solid lines are model correlations based on K–J model and the modified K–J model, respectively (Eqs. (4) and (5)) and all the correlation parameters are given in Table 3.

defining the mixture separation factor μ and the separation efficiency HE follows:

$$\mu = \frac{y_{31}}{y_{32}} \quad (8)$$

$$HE(\%) = \frac{y_{31}}{y_{31} + y_{32}} \times 100 \quad (9)$$

where y_{31} , y_{32} are the mole fraction solubility of *m*-NBA and 3,5-DNBA in the ternary system (3,5-DNBA + *m*-NBA + SCCO₂), respectively.

The separation factor is based upon the assumption that the solute molecules behave independently of each other. As shown in Table 2, the values of mixture separation factor μ range from 3.80 to 12.45. The separation factor μ isotherms of the mixture as a function of experimental pressure at different temperatures are shown in Fig. 4. As can be seen, the separation factor μ enhanced with increasing pressure at three temperatures. In the lower pressure region (less than 12 MPa), temperature is not the only factor; however, in the higher pressure region (more than 15 MPa), higher temperature enhanced the separating effect. So in a higher pressure region, higher temperature is a positive factor for the separation enhancement in this ternary system.

As shown in Table 2, the average value of HE is proximity to 90, which means that the purity of separation can be advanced to 90%. Thus, it could be applied in the separation of the mixture of 3,5-DNBA and *m*-NBA using SCCO₂ technology in the industry separation.

4.4. Model correlation

The correlated results and optimal parameters of the experimental solubility data using Chrastil model, the modified Adachi and Lu model, K–J model, and the modified K–J model, Eqs. (2)–(5), are listed in Table 3 and shown in Figs. 2 and 3. From Table 3, the solubility data of pure 3,5-DNBA and *m*-NBA in SCCO₂ are well correlated by all models, Eqs. (2)–(5), with the values of AARD of (3.20–5.03) and (5.10–9.51), respectively. The existence of the UCEP can be the reason why the correlated results of *m*-NBA with the different models are worse than that of 3,5-DNBA [10]. Compared with the binary system, for the ternary system, the solubility data of mixed 3,5-DNBA and *m*-NBA in SCCO₂ are not well correlated by all models, Eqs. (2)–(5), with the values of AARD of (8.54–12.81) and (8.58–12.25), respectively. The molecular interactions in the ternary system are more complicated than that in the binary

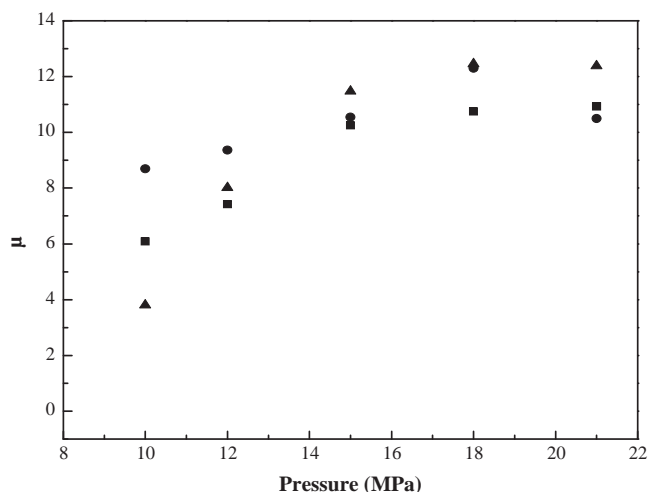


Fig. 4. Separation factor μ (Table 2) isotherms of mixture (3,5-DNBA + *m*-NBA) in SCCO_2 with pressure (■) 308 K; (●) 318 K; (▲) 328 K.

system, which may lead to the decline of relations degree and accuracy.

Comparing the values of AARD for all models in Table 3, the modified K–J model proposed in this work (Eq. (5)) correlates the solubility better, which is superior to the existing models, Eqs. (2)–(4). Furthermore, the solubility data of pure and mixed solid solutes in SCCO_2 are correlated better by the modified K–J model (Eq. (5)) and the modified Adachi and Lu model (Eq. (3)) than Chrastil model (Eq. (2)) and K–J model (Eq. (4)). From the expression of models and molecular structures of solid solutes, the reason may result from the complicity between the solubility of solid solutes and the density of CO_2 (ρ_1). Chrastil and K–J models (Eqs. (2) and (4)) illuminate that the relationship between the logarithm of solubility (S or y_2) and the solvent's density ($\ln \rho_1$ or ρ_1) is linear. However, the modified K–J and the modified Adachi and Lu models (Eqs. (3) and (5)) indicate the more complicated relationship between the solubility and the solvent's density. Therefore, the modified K–J and the modified Adachi and Lu models (Eqs. (3) and (5)) are more suitable to correlate the solubility data of solid solutes in SCCO_2 , especially the modified K–J model (Eq. (5)).

4.5. Verification of the modified K–J model

The solid solubility data of 23 different solid compounds in SCCO_2 were collected from literature [27–37], concluding 13 binary systems, 13 ternary systems, and 1 quaternary system. The solubility data were correlated with K–J model and the modified K–J model (Eqs. (4) and (5)). Table 4 shows the experimental conditions of these compounds from literature. The correlated parameters and results are shown in Tables 5 and 6 along with AARD. It is observed that the new proposed model (Eq. (5)) has successfully correlated the solubility data of all the compounds within 5.11% AARD. Comparing with the correlation result by K–J model (Eq. (4)) with 8.03% AARD, the modified K–J model (Eq. (5)) is superior to K–J model (Eq. (4)) for correlating the solubility of solid compounds in SCCO_2 . In addition, as shown in Table 6, for the binary system, the average AARD of the modified K–J model (Eq. (5)) is 5.26; for the ternary and quaternary systems, the average AARD is 5.04, which indicates that the modified K–J model (Eq. (5)) in this study is able to correlate the solubility data of pure and mixed solid compounds with less AARD. Table 6 also shows the comparison of the AARD obtained by the modified K–J model (Eq. (5)) and the models from literature. Therefore, the above results indicate the new proposed model (Eq. (5)) presents more accurate correlation

for solubility data of solid compounds in SCCO_2 , not only for the binary system (pure solute + SCCO_2), but also for the ternary system (mixed solutes + SCCO_2). It is an excellent practical model that could be employed to speed up the process of SCF applications in the industry.

5. Conclusions

In this work, the solubility of pure 3,5-DNBA and *m*-NBA and their equal-weight mixture in SCCO_2 was determined at 308, 318, and 328 K, over a pressure range from 10.0 to 21.0 MPa. The pressure and temperature effects on solubility in the ternary system were similar to those who obtained in the binary system. The higher polarity of 3,5-DNBA led to its lower solubility in SCCO_2 compared with *m*-NBA both in the binary and ternary systems.

In the ternary system, one solid solute played a “co-solvent” role, which resulted in a significant increase in the solubility of another solute. The effect of solubility enhancement *SE* has been observed. The average values of *SE* of 3,5-DNBA at 308, 318, and 328 K are up to 183, 118, and 67, respectively. And the corresponding values of *SE* of *m*-NBA are 30, 32, and 16, respectively. The results indicate that the solubility enhancement of 3,5-DNBA is higher than *m*-NBA in the ternary system. The mixture separation factor μ and the separation efficiency *HE* were investigated. The maximum values of μ and *HE* were 12.45 and 92.57, respectively, which indicate it is successful to separate the mixture of 3,5-DNBA and *m*-NBA using SCCO_2 technology.

The modified K–J model was proposed for correlating the solubility of solid compounds in SCCO_2 . The equilibrium solubility data of pure and mixed solutes in SCCO_2 were correlated by Chrastil model, the modified Adachi and Lu model, K–J model, and the modified K–J model with the values of AARD in ranging of (4.75–12.81), (3.20–8.71), (5.03–11.72), and (3.22–8.58), respectively. The modified K–J model proposed in this work correlates the solubility better, which is superior to another three models. Solubility data from 23 different solid compounds were taken from literature and correlated by K–J model and the modified K–J model in good accuracy. The total average values of AARD from K–J model and the modified K–J model were 8.03 and 5.11, respectively.

Acknowledgements

This research was financially supported by the funds awarded by National Natural Science Foundation of China (no. 20776006) and the supports from Petrochina Company Limited through the Applied Research ProProject (no. 2009A-3801-02). The authors are grateful to the support of this research from the Mass Transfer and Separation Laboratory in Beijing University of Chemical Technology.

References

- [1] R.B. Gupta, J.J. Shim, Solubilities in Supercritical Carbon Dioxide, CRC Press, Boca Raton, 2007.
- [2] J. Fages, H. Lochard, J.J. Letourneau, M. Sauceau, E. Rodier, Particle generation for pharmaceutical applications using supercritical fluid technology, Powder Technol. 141 (2004) 219–226.
- [3] G.B. Bachman, J.L. Dever, The $\text{BF}_3 \cdot \text{N}_2\text{O}_5$ complex. Its use as a nitrating agent, J. Am. Chem. Soc. 80 (1958) 5871–5873.
- [4] F.P. Lucien, N.R. Foster, Solubilities of solid mixtures in supercritical carbon dioxide: a review, J. Supercrit. Fluids 17 (2000) 111–134.
- [5] R.B. Gupta, J.J. Shim, Solubility in Supercritical Carbon Dioxide, CRC Press, New York, 2007.
- [6] C. Garlapati, G. Madras, New empirical expressions to correlate solubilities of solids in supercritical carbon dioxide, Thermochim. Acta 500 (2010) 123–127.
- [7] R. Ch, G. Madras, An association model for the solubilities of pharmaceuticals in supercritical carbon dioxide, Thermochim. Acta 507–508 (2010) 99–105.
- [8] K.G. Joback, R.C. Reid, Estimation of pure component properties from group-contributions, Chem. Eng. Commun. 57 (1987) 233–243.

- [9] R.C. Reid, J.M. Prausnitz, B.E. Poling, *The Properties of Gases and Liquids*, McGraw-Hill, New York, 1988.
- [10] A. Taberner, E.M.M. del Valle, M.A. Galan, A comparison between semiempirical equations to predict the solubility of pharmaceutical compounds in supercritical carbon dioxide, *J. Supercrit. Fluids* 52 (2010) 161–174.
- [11] J. Chrastil, Solubility of solids and liquids in supercritical gases, *J. Phys. Chem.* 86 (1982) 3016–3021.
- [12] J. Mendez-Santiago, A.S. Teja, The solubility of solids in supercritical fluids, *Fluid Phase Equilib.* 158 (1999) 501–510.
- [13] K.D. Bartle, A.A. Clifford, S.A. Jafar, G.F. Shilstone, Solubilities of solids and liquids of low volatility in supercritical carbon dioxide, *J. Phys. Chem. Ref. Data* 20 (1991) 201–219.
- [14] M.D. Gordillo, M.A. Blanco, A. Molero, E. Martinez de la Ossa, Solubility of the antibiotic penicillin G in supercritical carbon dioxide, *J. Supercrit. Fluids* 15 (1999) 183–190.
- [15] J.M. del Valle, J.M. Aguilera, An improved equation for predicting the solubility of vegetable oils in supercritical CO₂, *Ind. Eng. Chem. Res.* 27 (1988) 1551–1553.
- [16] Y. Adachi, B.C.Y. Lu, Supercritical fluid extraction with carbon dioxide and ethylene, *Fluid Phase Equilib.* 14 (1983) 147–156.
- [17] D.L. Sparks, R. Hernandez, L.A. Estevez, Evaluation of density-based models for the solubility of solids in supercritical carbon dioxide and formulation a new model, *Chem. Eng. Sci.* 63 (2008) 4292–4301.
- [18] S.K. Kumar, K.P. Johnston, Modelling the solubility of solids in supercritical fluids with density as the independent variable, *J. Supercrit. Fluids* 1 (1988) 15–22.
- [19] Z. Yu, B. Singh, S.S.H. Rizvi, J.A. Zolleweg, Solubilities of fatty acids, fatty acid esters, and fats and oils in supercritical CO₂, *J. Supercrit. Fluids* 7 (1994) 51–59.
- [20] G.H. Tian, J.S. Jin, Z.T. Zhang, J.J. Guo, Solubility of mixed solids in supercritical carbon dioxide, *Fluid Phase Equilib.* 251 (2007) 47–51.
- [21] J.L. Li, J.S. Jin, Z.T. Zhang, X.M. Pei, Solubility of *p*-toluenesulfonamide in pure and modified supercritical carbon dioxide, *J. Chem. Eng. Data* 54 (2009) 1142–1146.
- [22] S. Grabowski, R.G. Delaplane, I. Olovsson, Crystal and molecular structure of phenazine-3, 5-dinitrobenzoic acid complex, C₁₂H₈N₂-C₇H₄O₆N₂, *J. Mol. Struct.* 597 (2001) 67–71.
- [23] E.J. Beckman, Supercritical and near-critical CO₂ in green chemical synthesis and processing, *J. Supercrit. Fluids* 28 (2004) 121–191.
- [24] M. McHugh, M.E. Paulaitis, Solid solubilities of naphthalene and biphenyl in supercritical carbon dioxide, *J. Chem. Eng. Data* 25 (1980) 326–329.
- [25] R.T. Kurnik, R.C. Reid, Solubility of solid mixtures in supercritical fluids, *Fluid Phase Equilib.* 8 (1982) 93–105.
- [26] F.P. Lucien, N.R. Foster, Solubility of mixed hydroxybenzoic acid isomers in supercritical carbon dioxide, *J. Chem. Eng. Data* 43 (1998) 726–731.
- [27] G.H. Tian, J.S. Jin, J.J. Guo, Z.T. Zhang, Mixed Solubilities of 5-sulfosalicylic acid and *p*-aminobenzoic acid in supercritical carbon dioxide, *J. Chem. Eng. Data* 52 (2007) 1800–1802.
- [28] W.M. Li, J.S. Jin, G.H. Tian, Z.T. Zhang, Single-component and mixture solubilities of ethyl *p*-hydroxybenzoate and ethyl *p*-aminobenzoate in supercritical CO₂, *Fluid Phase Equilib.* 264 (2008) 93–98.
- [29] J.L. Li, J.S. Jin, Z.T. Zhang, X.M. Pei, Equilibrium solubilities of a *p*-toluenesulfonamide and sulfanilamide mixture in supercritical carbon dioxide with and without ethanol, *J. Supercrit. Fluids* 52 (2010) 11–17.
- [30] S. Raviapaty, K.J. Koebke, D.J. Chesney, Polar mixed-solid solute systems in supercritical carbon dioxide: entrainer effect and its influence on solubility and selectivity, *J. Chem. Eng. Data* 53 (2008) 415–421.
- [31] M.A. Khiavi, Y. Yamini, M.A. Farajzadeh, Solubilities of two steroid drugs and their mixtures in supercritical carbon dioxide, *J. Supercrit. Fluids* 30 (2004) 111–117.
- [32] P. Dong, M.X. Xu, X.Y. Lu, C.M. Lin, Measurement and correlation of solubilities of C.I. Disperse Red 73, C. I. Disperse Yellow 119 and their mixture in supercritical carbon dioxide, *Fluid Phase Equilib.* 297 (2010) 46–51.
- [33] Z. Huang, M. Feng, Y.H. Guo, J.F. Su, L.J. Teng, T.Y. Liu, Y.C. Chiew, Ternary solubility of mixed cholesteryl esters in supercritical carbon dioxide, *Fluid Phase Equilib.* 272 (2008) 8–17.
- [34] G. Paniri, H.S. Ghaziaskar, M. Rezaayat, Ternary solubility of mono- and di-tert-butyl ethers of glycerol in supercritical carbon dioxide, *J. Supercrit. Fluids* 55 (2010) 43–48.
- [35] W.J. Cross, A. Akgerman, Single-component and mixture solubilities of hexachlorobenzene and pentachlorophenol in supercritical carbon dioxide, *Ind. Eng. Chem. Res.* 37 (1998) 1510–1518.
- [36] K.J. Pennisi, E.H. Chimowitz, Solubilities of solid 1,10-decanediol and a solid mixture of 1,10-decanediol and benzoic acid in supercritical carbon dioxide, *J. Chem. Eng. Data* 31 (1986) 285–288.
- [37] E. Kosal, G.D. Holder, Solubility of anthracene and phenanthrene mixtures in supercritical carbon dioxide, *J. Chem. Eng. Data* 32 (1987) 148–150.